Supporting Information for

Interfacial effects in CuO/Co_3O_4 heterostructures enhance benzene catalytic oxidation performance

Qun Li[a, f], Ningjing Luo[b, f], Dong Xia[a], Peng Huang[c], Xiaobin Liu[d], Tareque Odoom-Wubah[a], Jiale Huang[a], Guoliang Chai[b], Daohua Sun[a], Qingbiao Li[a, e*]*

[a] Department of Chemical and Biochemical Engineering, College of Chemistry and Chemical Engineering, Xiamen University, Xiamen 361005, PR China

[b] State Key Laboratory of Structural Chemistry, Fujian Institute of Research on the Structure of Matter, Chinese Academy of Sciences (CAS), Fuzhou, 350002 Fujian, China.

[c] Department of Materials, University of Manchester, Manchester, M13 9PL, UK

[d] Environmental Science Research Center, College of the Environment & Ecology, Xiamen University, Xiamen 361005, P. R. China

[e] College of Food and Biological Engineering, Jimei University, Xiamen 361021, PR China

[f] These authors contributed equally: Qun Li, Ningjing Luo.

Corresponding authors: Daohua Sun, sdaohua@xmu.edu.cn; Qingbiao Li, kelqb@xmu.edu.cn

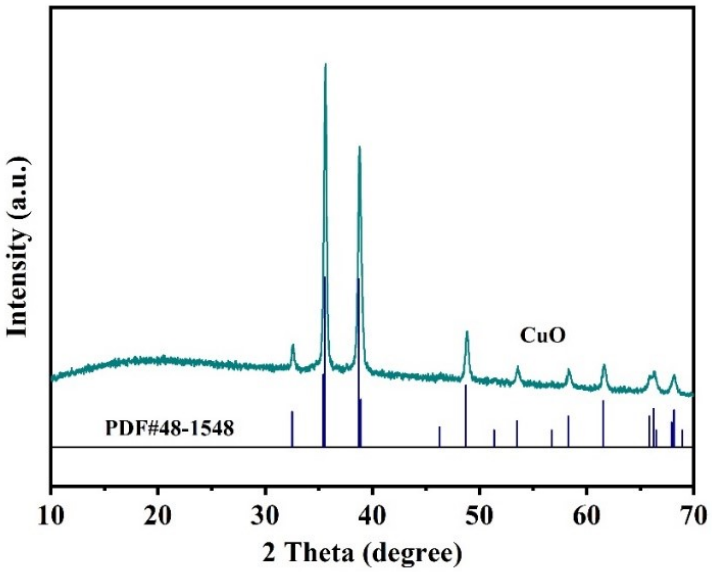

Figure S1. XRD pattern of CuO.

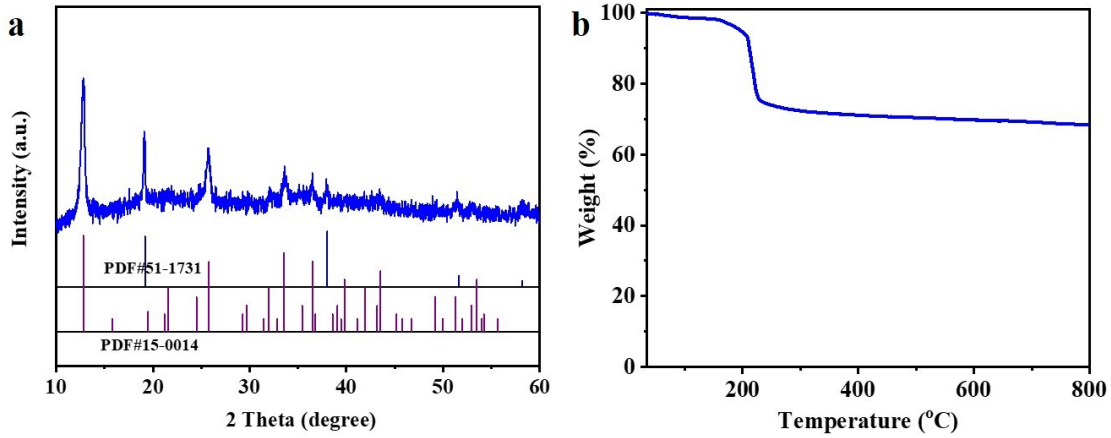

Figure S2. (a) XRD and (b) TGA pattern of CuCo-precursor.

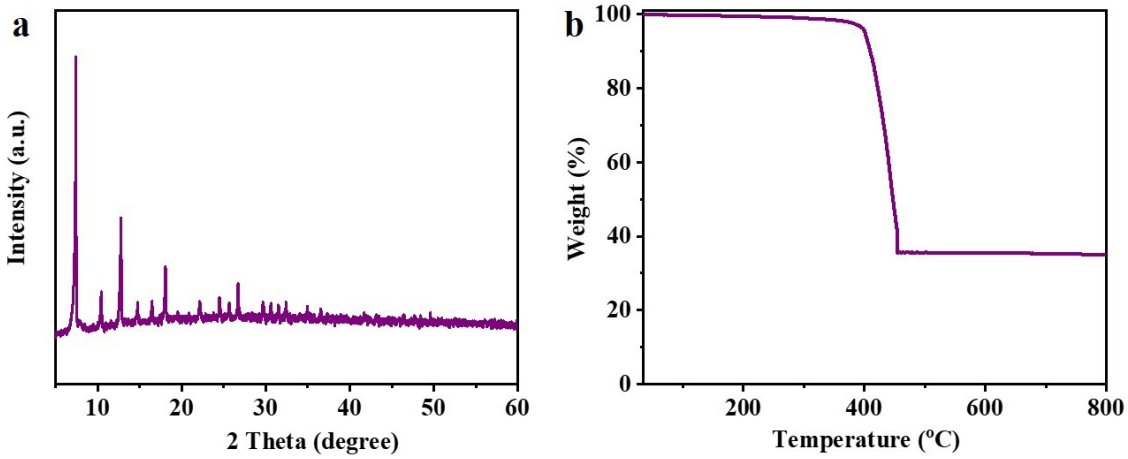

Figure S3. (a) XRD and (b) TGA pattern of ZIF-67.

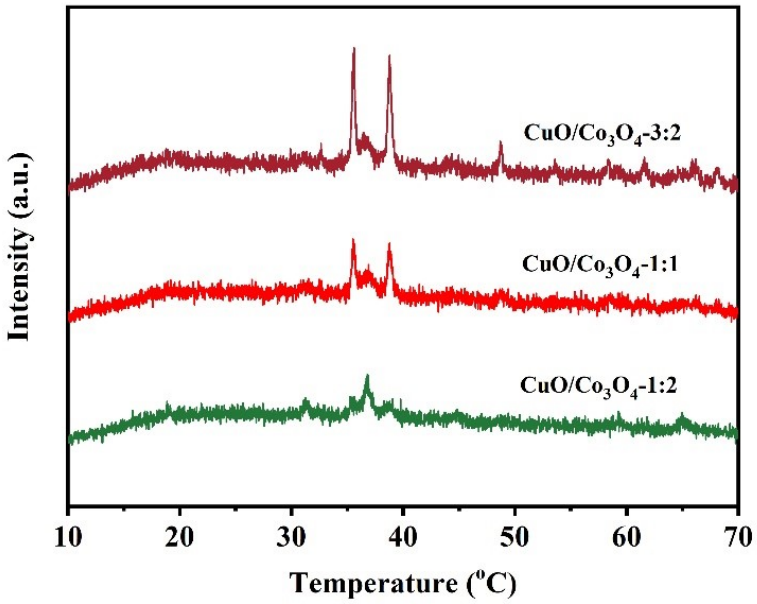

Figure S4. XRD patterns of CuO/Co_3O_4 with different Cu:Co ratio.

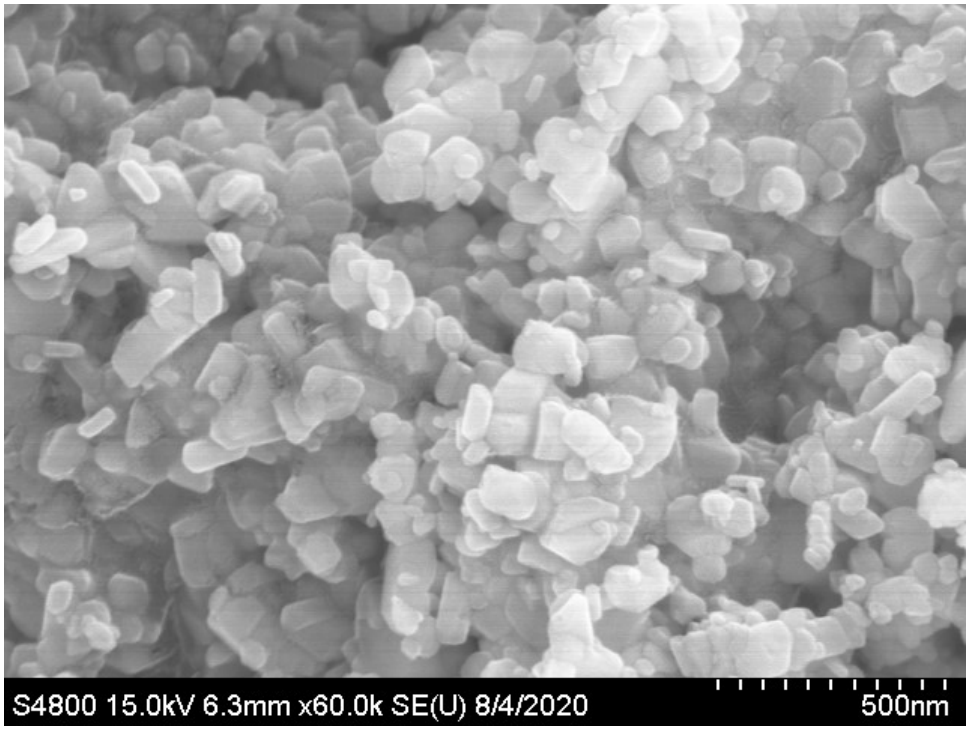

Figure S5. SEM image of CuO.

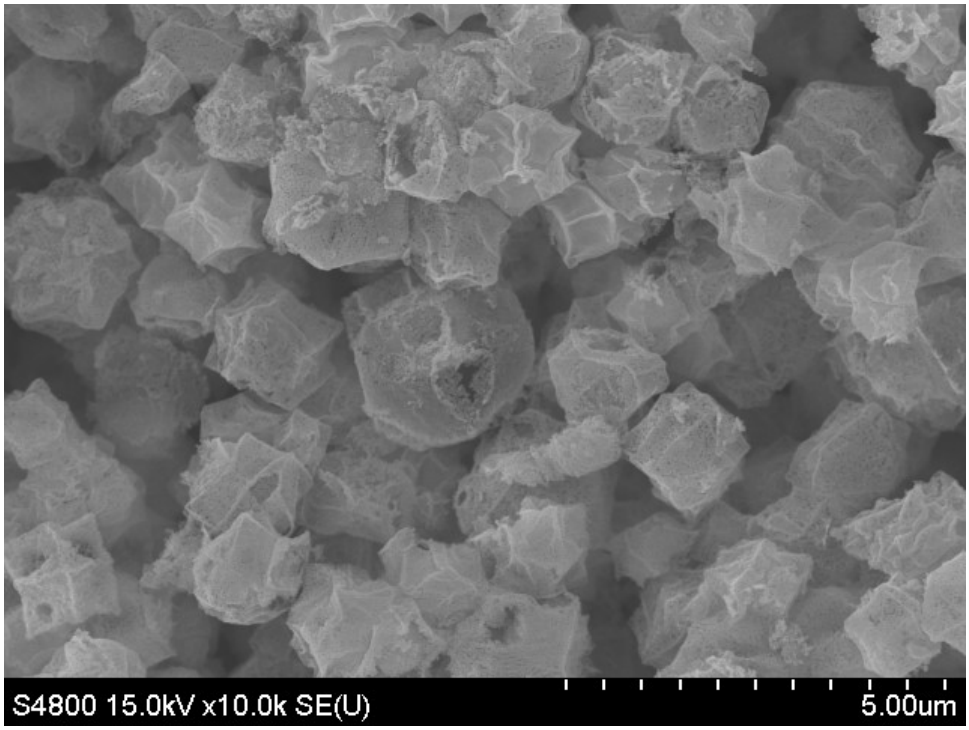

Figure S6. SEM image of ZIF-67 derived Co_3O_4.

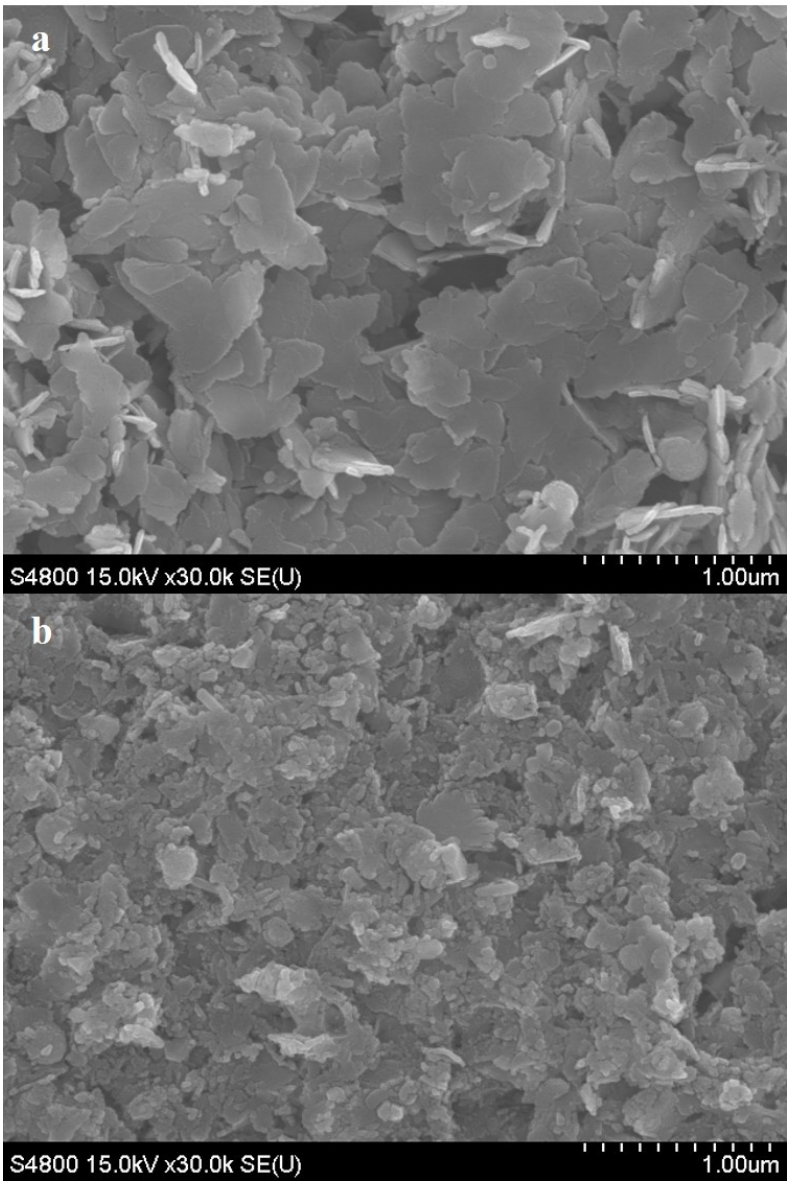

Figure S7. (a, b) SEM images of CuCo-precursor and CuO/Co_3O_4.

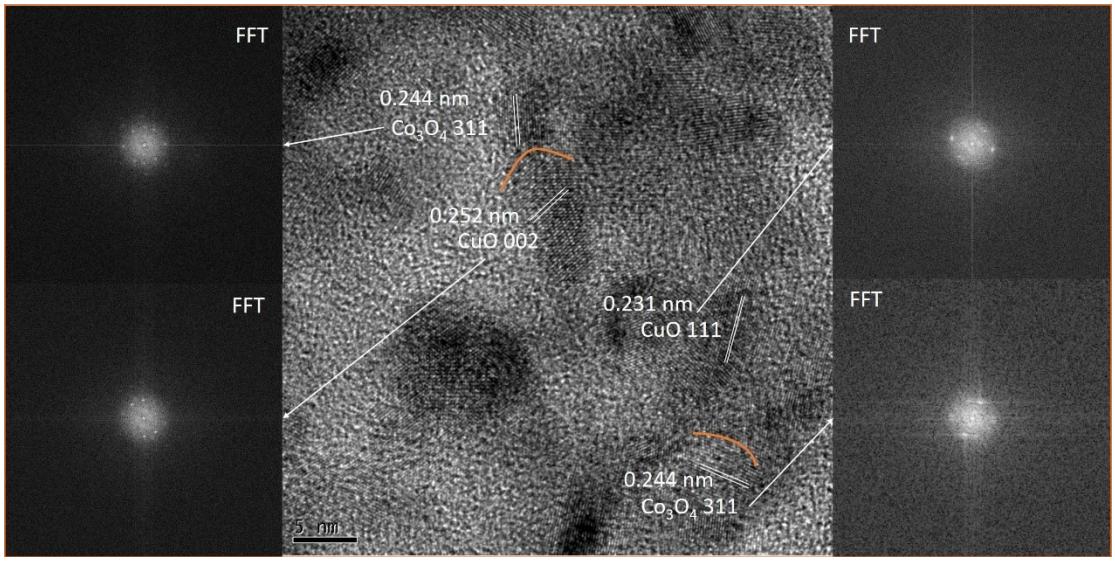

Figure S8. HRTEM image of CuO/Co_3O_4.

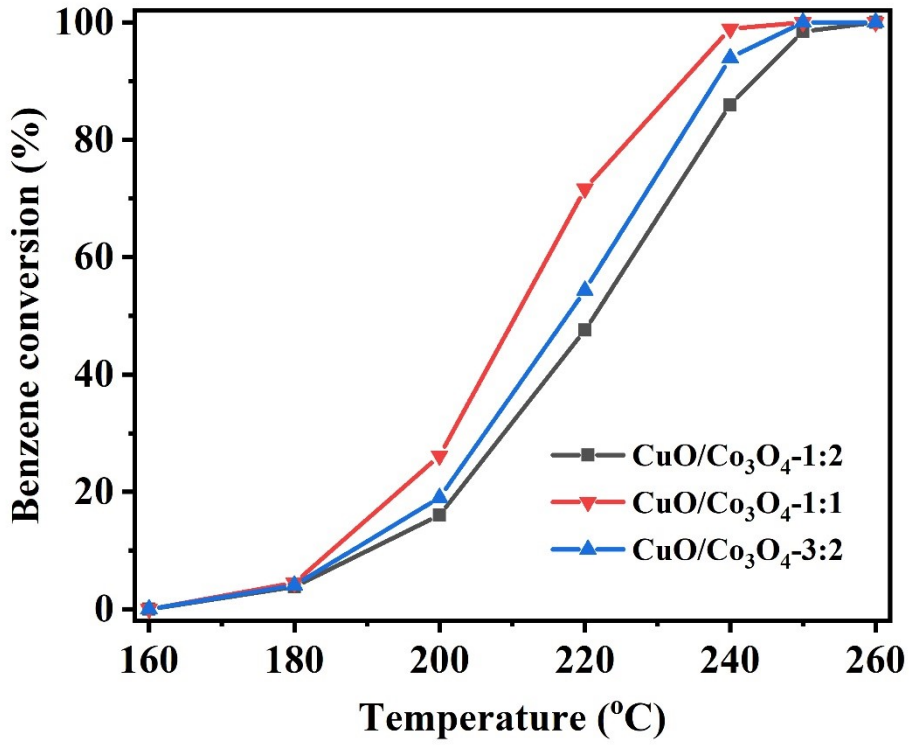

Figure S9. Benzene catalytic oxidation performance over CuO/Co_3O_4 catalysts with different molar ratios of Cu:Co.

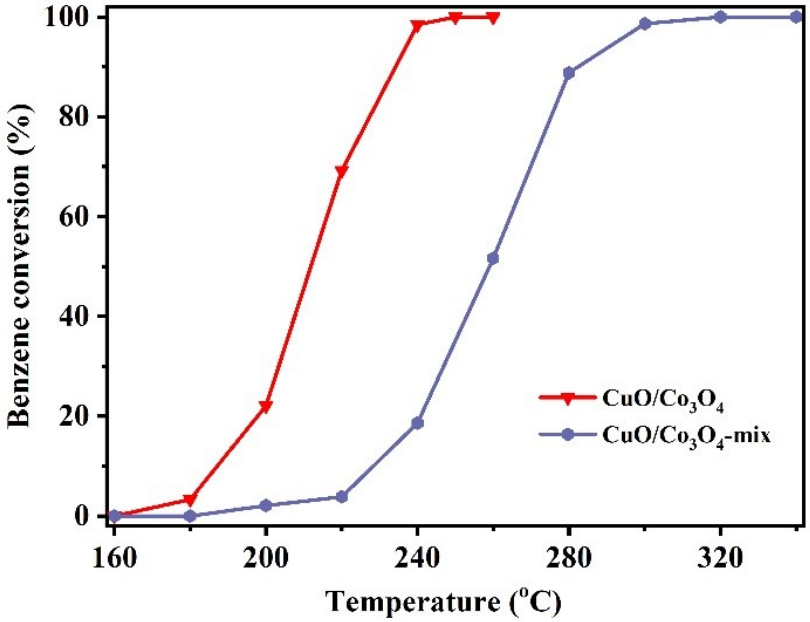

Figure S10. Comparison of the catalytic performance between the as-prepared CuO/Co_3O_4 and CuO/Co_3O_4-mix catalysts under the high SV of 120000 h^{-1}.

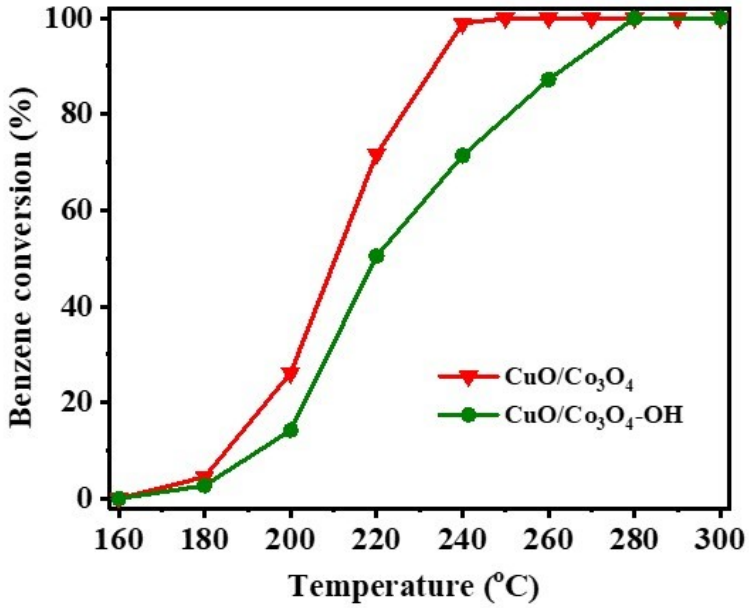

Figure S11. Catalytic benzene oxidation over CuO/Co_3O_4 and CuO/Co_3O_4-OH under the SV of 60000 h^{-1}.

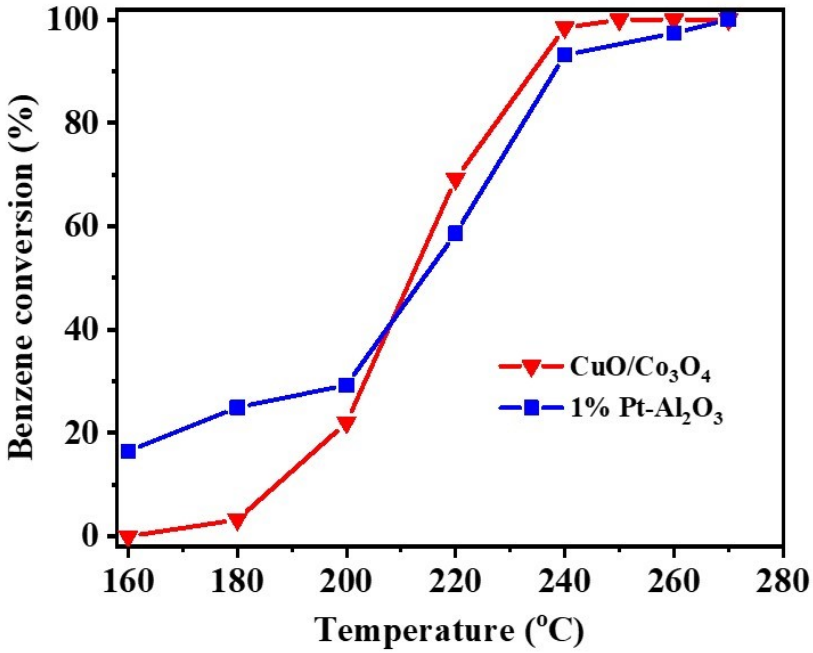

Figure S12. Comparison of the catalytic performance between the as-prepared CuO/Co_3O_4 and 1% $Pt\text{-}Al_2O_3$ catalysts under the high SV of 120000 h^{-1}.

Table S1. BET surface area, pore diameter and pore volume of the catalysts.

Sample	BET surface area (m^2/g)	Pore diameter (nm)	Pore volume (cm^3/g)
CuO/Co_3O_4-1:2	55	22.2	0.25
CuO/Co_3O_4-2:3	51	13.5	0.15
CuO/Co_3O_4-1:1	60	16.6	0.19
CuO	7	30.2	0.03
Co_3O_4	16	30.1	0.09

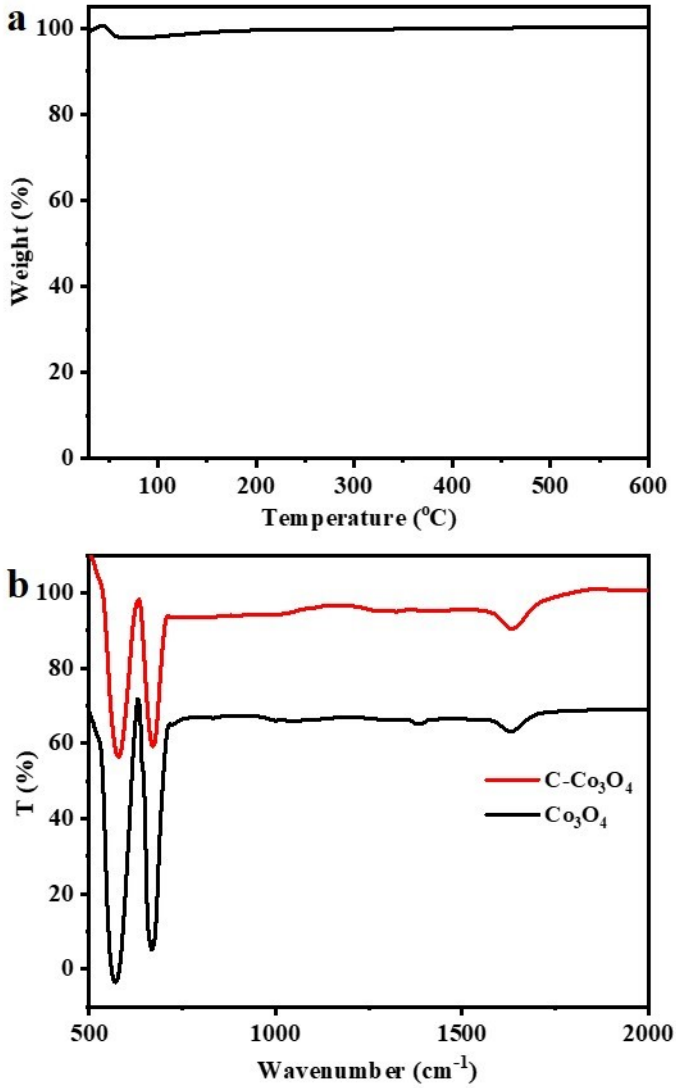

Figure S13. (a) TGA curve of the as-obtained Co_3O_4 catalyst, (b) FTIR spectra of the as-obtained Co_3O_4 and commercial Co_3O_4 catalysts (C-Co_3O_4).

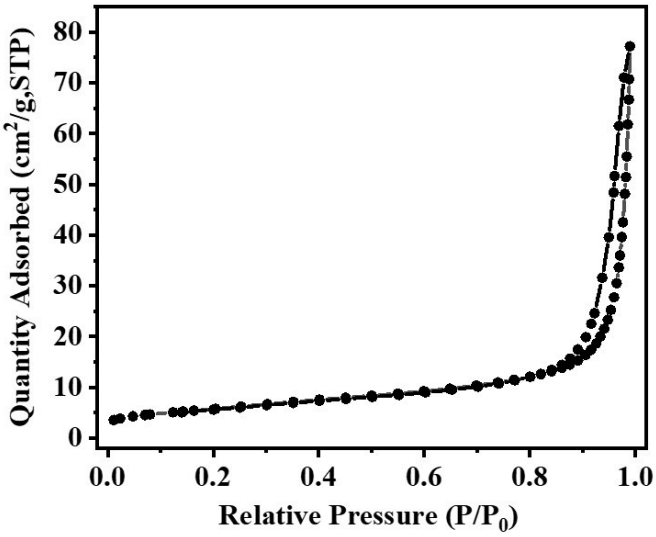

Figure S14. Re-tested N_2 adsorption-desorption isotherms of the Co_3O_4 catalysts.

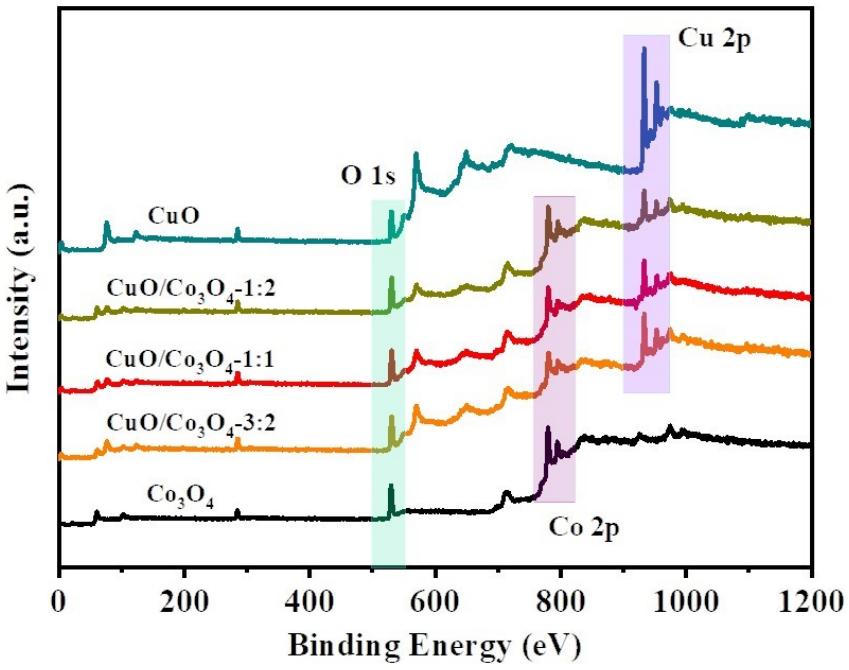

Figure S15 (amended). XPS survey scans of different catalysts.

Table S2. Surface elemental compositions of the as-prepared catalysts.

Catalyst	$O_{ads}/(O_{ads}+O_{latt})$	$Cu^{2+}/(Cu^{2+}+Cu^{+})$	$Co^{3+}/(Co^{3+}+Co^{2+})$
CuO/Co_3O_4-1:2	0.507	0.430	0.553
CuO/Co_3O_4-3:2	0.534	0.444	0.566
CuO/Co_3O_4-1:1	0.569	0.452	0.583
CuO	0.368	0.398	-
Co_3O_4	0.511	-	0.512

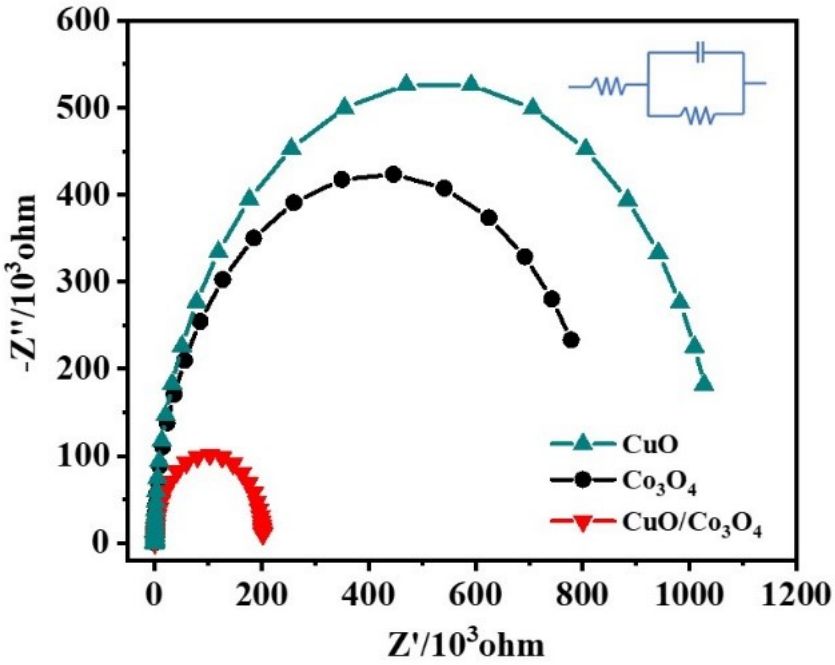

Figure S16 (amended). EIS curve of CuO, Co_3O_4, and CuO/Co_3O_4.

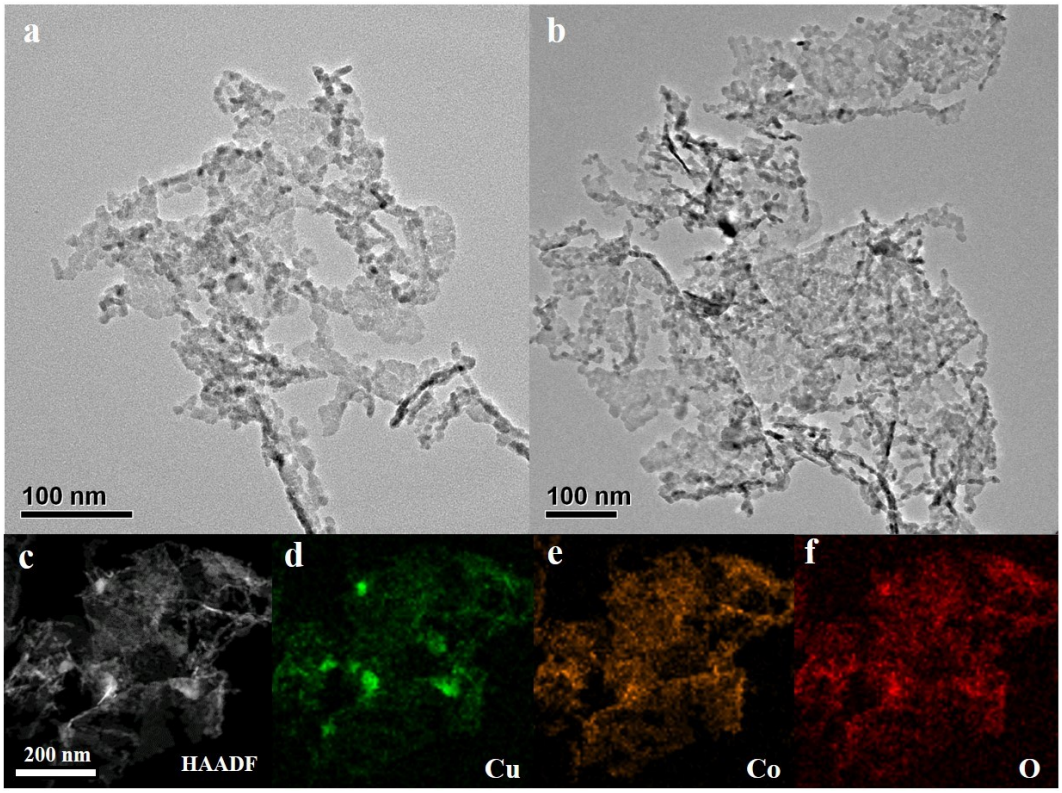

Figure S17. (a, b) TEM images of CuO/Co_3O_4 before and after 100h stability test. (c) HAADF images of CuO/Co_3O_4 after 100 h stability test, elemental mapping scan of (d) Cu, (e) Co and (f) O.

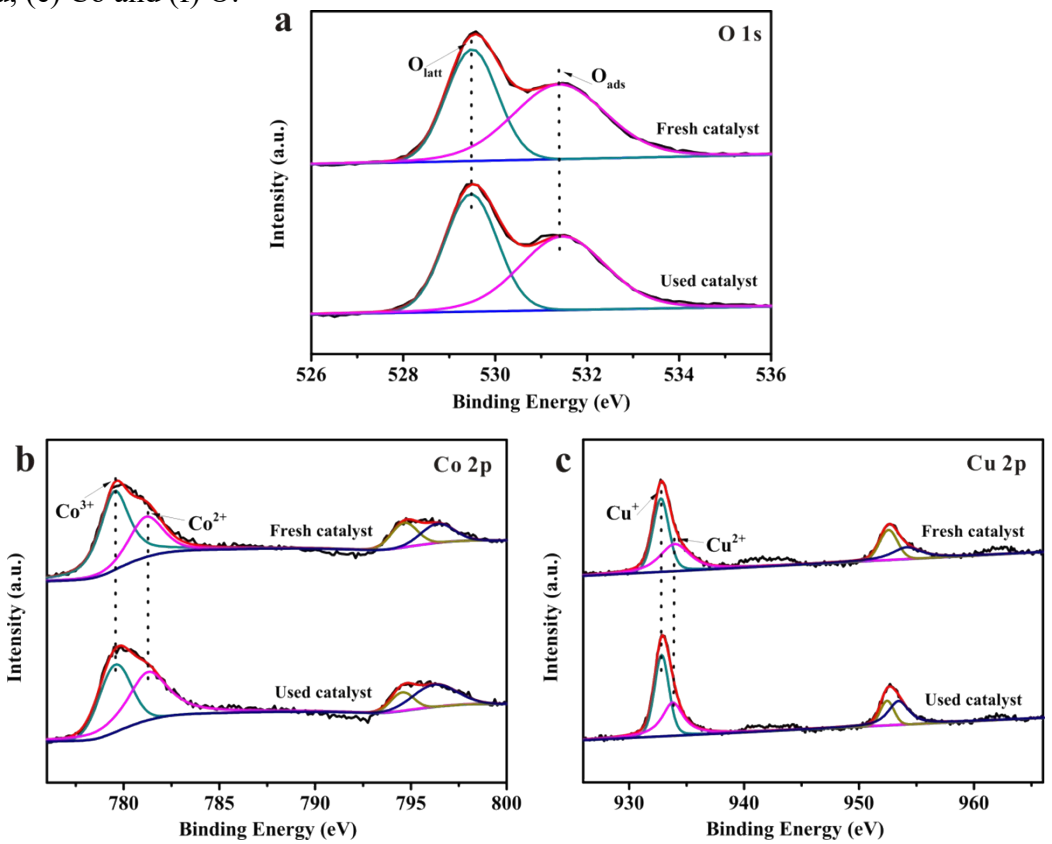

Figure S18. XPS spectra of (a) O 1s (b) Co 2p and (c) Cu 2p before and after 100 h stability test.

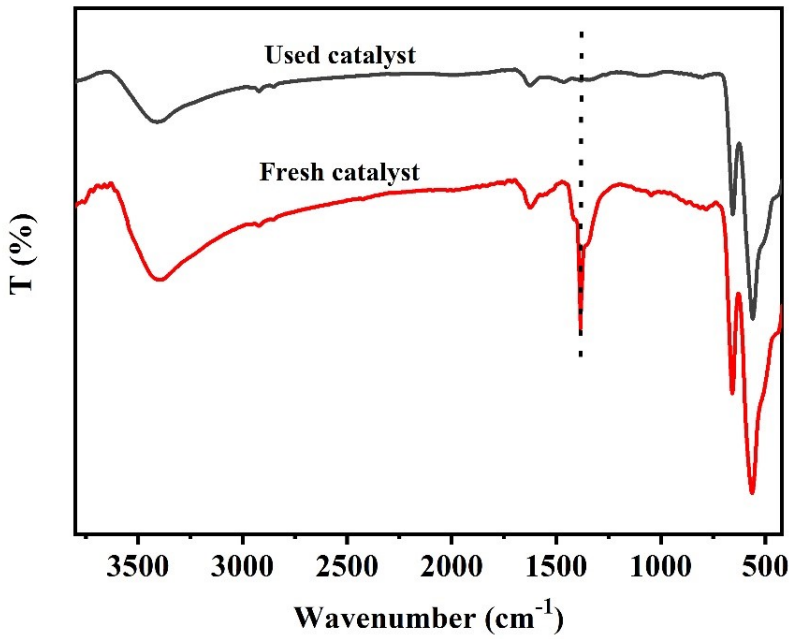

Figure S19. FTIR spectra of the fresh and used catalysts.

To illustrate the origin of the CuO/Co_3O_4 catalyst composition in the benzene oxidation process, we assumed two boundary conditions of doping minimum Cu and Co concentrations (2 % and 0.8 %, respectively). The first boundary condition is that one Cu atom replaces the Co atom on the superficial surface of Co_3O_4 (311) surface, which also leads to a maximum Co concentration. While the other is that one Co atom replaces one Cu atom on the most superficial CuO (111) surface, resulting in a maximum Cu concentration and lowest Co concentration. Importantly, all potential doped Co_3O_4 (311) and CuO (111) structures were considered, aiming to screen out the most stably doped structures. After that, the benzene adsorption processes were correspondingly studied on the most stable Cu/Co_3O_4 (311) surface and Co/CuO (111) surface.

For the minimum Co concentration in the Cu/Co_3O_4 composition (0.8 %), the adsorption energy of benzene on pure CuO (111) is 0.18 eV, while the adsorption energy of benzene on Co/CuO (111) has decreased by 1.3 eV to -1.18 eV. Clearly, the small amount of Co (0.8 %) is more effective for the reduction of adsorption energy than 2% Cu doping.

The electronic structures of Co/CuO (111) have also been calculated and shown in Figure 8g and Figure S14. Similarly, Co atom in the Co/CuO (111) surface also facilitates the electron accumulation, and the corresponding charge density differences

of Co/CuO (111) surface indicates that the adjacent O atoms and Cu atoms around the Co atom on the Co/CuO (111) surface obtain electron from the doped Co atom (Figure 11g). Compared with Cu/Co_3O_4 (311) surface (Figure S14), the PDOS of benzene after Co-doping also shift downs along the Fermi level but deeper than the pure CuO (111) surface, which indicates Co-doping could effectively strengthen the benzene adsorption. Besides, the total density of states (TDOS) of the superficial Cu atoms and O atoms also represent more obvious movement.

The above DFT results illustrate that the synthesized material with small amounts of atomic doping on catalyst surface bbring better catalyst properties than the pure surface. Essentially speaking, the pure Co_3O_4 (311) surface presented a better catalytic performance in benzene oxidation than that of the pure CuO (111) surface, due to a lower adsorption energy of -1.39 eV (v.s. 0,18 eV for the CuO (111) surface). This fact is further proved by better performance improvement in Co-doping of CuO (111) surface. As a result, utilizing Cu-doping in the Co_3O_4 surface is an important approach to enhance the catalytic benzene oxidation performance.

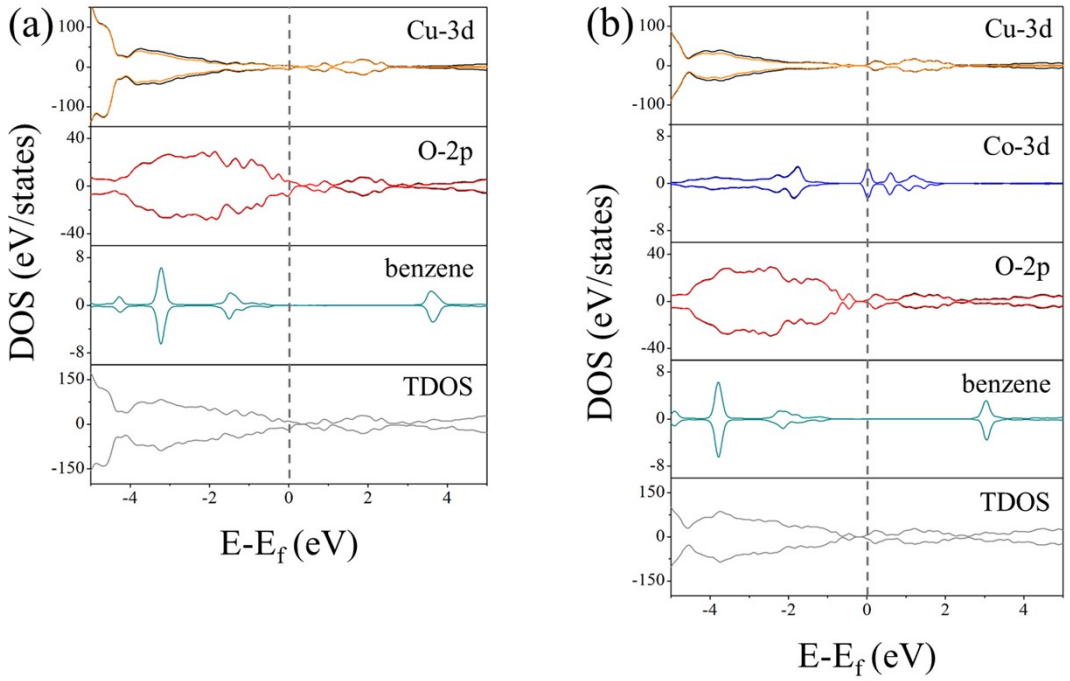

Figure S20. The partial density of states (PDOS) of benzene adsorbed on pure CuO (111) surface and Co/CuO (111) surface. Those dotted lines mean the Fermi level. The black lines in the PDOS of Co, Cu, and O correspond to the total density of states (TDOS) of Co, Cu, and O.

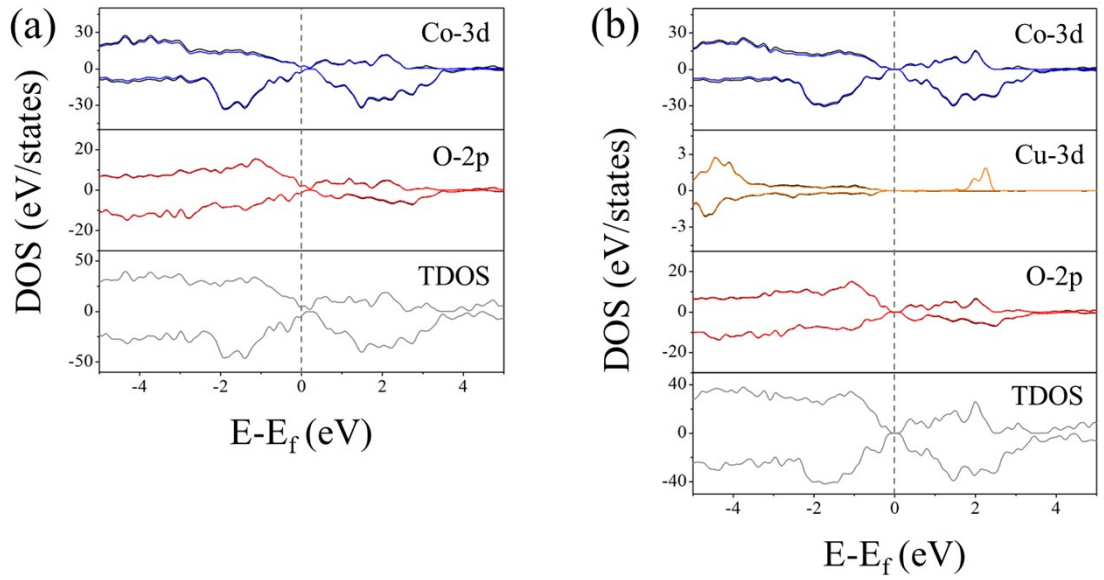

Figure S21. The partial density of states (PDOS) of pure Co_3O_4 (311) surface and Cu/Co_3O_4 (311) surface. Those dotted lines mean the Fermi level. The black lines in the PDOS of Co, Cu, and O correspond to the total density of states (TDOS) of Co, Cu, and O.

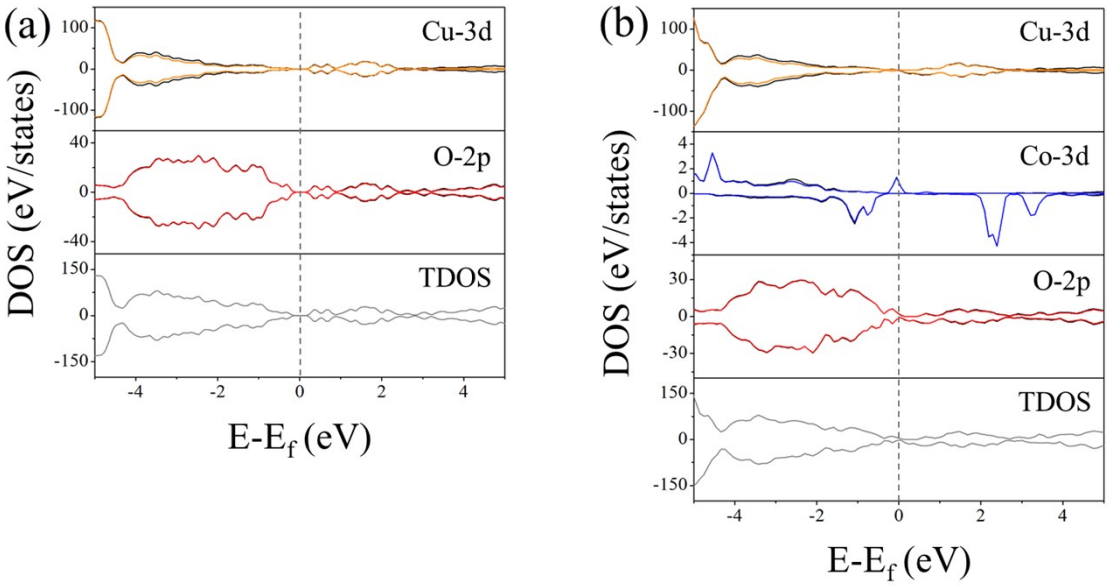

Figure S22. The partial density of states (PDOS) of pure CuO (111) surface and Co/CuO (111) surface. Those dotted lines mean the Fermi level. The black lines in the PDOS of Co, Cu, and O correspond to the total density of states (TDOS) of Co, Cu, and O.

Table S3. The calculated magnetic moments of Cu/Co_3O_4 (311) surface and Co/CuO (111) surface. The unit of magnetic moments is μ_B。

Doped-atom	magnetic moment
Co	-0.655
Cu	2.626